Marine Biology (2001) 138: 717–730

S. Johnsen · E. A. Widder

Ultraviolet absorption in transparent zooplankton and its implications for depth distribution and visual predation

Received: 14 April 2000 / Accepted: 16 November 2000

Abstract The use of transparency as camouflage in the epipelagic realm is complicated by the presence of ultraviolet radiation, because the presence of UV-protective pigments decreases UV transparency and may reveal transparent zooplankton to predators and prey with UV vision. During July 1999, September 1999, and June 2000, transparency measurements (from 280 to 500 nm) were made on living specimens of 15 epipelagic (collection depth: 0–20 m, average: 11 ± 1 m) and 19 mesopelagic (collection depth: 150–790 m, average: 370 ± 40 m) species of transparent zooplankton from Oceanographer Canyon and Wilkinson Basin in the Northwest Atlantic Ocean. In addition, measurements of downwelling irradiance (from 330 to 500 nm) versus depth were made. The tissues from epipelagic zooplankton had lower UV transparency than those from mesopelagic zooplankton, while the average visible transparency (at 480 nm) of the two groups was not significantly different. Percent transparency was positively correlated with wavelength over most of the measured range, with a rapid decrease below a certain cutoff wavelength. In mesopelagic tissues, the cutoff wavelength was generally 300 nm. In epipelagic tissues, the cutoff wavelength was between 300 and 400 nm. Twelve out of 19 epipelagic tissues had transparencies at 320 nm that were half or less than their 480 nm transparency values, versus only 4 out of 21 mesopelagic tissues. The effects of UV absorption on UV visibility and minimum attainable depth were modeled using contrast theory and the physics of light attenuation. Because UV absorption was generally significantly greater in the UVB than in the UVA spectrum (where UV vision occurs), and because the highest UV absorption was often found in less transparent individuals, its modeled effects on visibility were slight compared to its effects on minimum attainable depth.

Communicated by J. P. Grassle, New Brunswick

S. Johnsen (✉)
Biology Department, MS #33,
Woods Hole Oceanographic Institution,
Woods Hole, MA 02543-1049, USA

e-mail: sjohnsen@whoi.edu
Tel.: +1-508-2893603; Fax: +1-508-4572134

E. A. Widder
Marine Science Division,
Harbor Branch Oceanographic Institution,
Fort Pierce, Florida, USA

Introduction

Two striking characteristics of many oceanic zooplankton are their delicacy and their high degree of exposure to visual predators and prey. Transparency is one of the most common adaptations to this environment and appears to have evolved many times in parallel. All major pelagic phyla have transparent representatives, and many taxonomic groups (cnidarians, ctenophores, chaetognaths, polychaetes, salps, doliolids, cranchid squid, pseudothecosomate pteropods, heteropods, hyperiid amphipods) are dominated by transparent forms (McFall-Ngai 1990; Hamner 1996; Johnsen and Widder 1998; Johnsen 2000). Many species achieve nearly complete invisibility, and it has long been assumed that transparency functions as camouflage (Hobson and Chess 1978; McFall-Ngai 1990).

Although transparent, mostly gelatinous zooplankton are poorly represented in trawls, research using blue-water diving techniques and submersibles has shown that they are diverse, abundant, and play critical roles as herbivores, predators and prey of zooplankton and ichthyoplankton, and conveyers of organic mass to deeper waters (e.g. Hamner et al. 1975; Alldredge and Madin 1982; Alldredge 1984; Caron et al. 1989; Lalli and Gilmer 1989; Pages et al. 1996; Madin et al. 1997; Purcell 1997). All pelagic phyla contain numerous transparent species that either prey on, or are preyed upon by species with well-developed visual systems (reviewed by Johnsen and Widder 1998). In addition, many

of these species (e.g. cnidarians, ctenophores, and chaetognaths) prey upon copepods and larval crustaceans (Baier and Purcell 1997; Harbison et al. 1978), which react defensively to shadows (Forward 1976; Buskey et al. 1986) and thus may react to opaque or translucent predators passing overhead.

Since the majority of transparent zooplankton are more delicate and less agile than their visually orienting predators or prey, their success in predator/prey interactions with these species depends critically upon their visibility and, in particular, their sighting distance (the maximum distance at which they are detectable by an organism relying on visual cues) (Johnsen and Widder 1998). Because underwater sighting distances are short, they are generally determined more by an object's contrast than by its size (Mertens 1970). An object's contrast depends on its distance from the viewer, its transparency, and the transparency of the surrounding water. Beyond the sighting distance, the object's contrast drops below what the viewer can detect. Because the sighting distance depends on the optical properties of the zooplankton and the surrounding water, changes in either affect predator–prey relationships and possibly the species composition of the ecosystem (Zaret and Kerfoot 1975; Greene 1983; reviewed by McFall-Ngai 1990).

The issue of ultraviolet (UV) transparency is particularly intriguing. Recent research has shown that UV radiation is more abundant in epipelagic ecosystems (defined in this paper as the depth range 0–20 m) than previously supposed (Fleischmann 1989; Frank and Widder 1996; reviewed by El-Sayed et al. 1996 and Losey et al. 1999). This presents two problems for zooplankton that have evolved a concealment strategy based on transparency. The first involves UV vision among potential predators and prey. UV vision has been demonstrated in many marine species, and it has been conservatively estimated that there is sufficient UV light for vision down to 200 m in clear ocean water (reviewed by Shashar 1995 and Losey et al. 1999). Visual pigments with UV sensitivity (though not necessarily peaking in the UV) have been found in the Atlantic halibut (Helvik et al., in preparation), 22 (out of 41 examined) species of coral reef fish (McFarland and Loew 1994; McFarland et al., in preparation), juvenile salmonids (Bowmaker and Kunz 1987; Coughlin and Hawryshyn 1994), and decapod and stomatopod crustaceans (Cronin and Frank 1996; Marshall and Oberwinkler 1999). In addition, Siebeck and Marshall (2001) examined the lenses and corneas of 211 species of coral reef fish and found that 50% had high transparency at UV wavelengths. Since the majority of the lenses and corneas in high UV environments have high UV absorption (presumably to protect the retina from radiation damage) (Thorpe et al. 1993), Siebeck and Marshall suggest that ocular UV transparency often implies UV vision, particularly since in their study it is correlated with UV body coloration. Many researchers have suggested that further investigation will demonstrate that UV vision is widespread in the marine environment (McFarland 1991; Shashar 1995; Losey et al. 1999). Indeed, among freshwater teleosts UV vision appears to be fairly widespread (reviewed by Jacobs 1992, Goldsmith 1994, and Shashar 1995; Carleton et al. 2000). Several researchers have hypothesized that UV vision is primarily used to improve detection of planktonic prey (Loew et al. 1993; Cronin et al. 1994; McFarland and Loew 1994), and Browman et al. (1994) have shown that the presence of UV light improves the search behavior of certain UV-sensitive zooplanktivorous fish. The presence of UV sensitivity in planktivorous but not in non-planktivorous life stages of salmonids (reviewed by Tovee 1995), the correlation between UV vision and planktivory in coral reef fish (McFarland et al., in preparation), and the correlation between ocular UV transparency and planktivory (Siebeck and Marshall 2001) all suggest that UV vision is often used to increase the contrast of planktonic prey.

The second problem related to UV radiation is potential radiation damage. Numerous studies have shown that pelagic organisms are damaged by UV radiation in various ways, including deleterious effects on DNA, proteins, tissue, activity, growth, reproduction, and chemical defenses (Damkaer et al. 1980, 1981; Worrest 1982; Häder and Worrest 1991; Smith et al. 1992; Cronin and Hay 1995; El-Sayed et al. 1996; Hay 1996). Differential levels of these effects have been shown to influence biomass, sex ratios, and species compositions of both terrestrial and marine ecosystems (Bogenrieder and Klein 1982; Bothwell et al. 1994; Chalker-Scott 1995; Wängberg et al. 1996; Odmark et al. 1998). These effects are primarily due to UVB radiation (280–320 nm), and in clear polar water have been observed to depths of 20–25 m (reviewed by El-Sayed et al. 1996). At lower latitudes, where surface UV irradiance is higher, these effects are likely to be observed even deeper.

One of the primary defensive mechanisms against UV radiation damage is the use of UV-absorbing pigments (Dunlap et al. 1991; Douglas and Thorpe 1992; Thorpe et al. 1993; Karentz 1994; Carroll and Shick 1996; Hannach and Sigelo 1998). However, because UV-protective pigments must attenuate UV light to be effective, their presence reduces an organism's transparency in the UV, and thus increases its sighting distance for predators and prey with UV vision. This presents a potential dilemma for transparent epipelagic zooplankton: protection or concealment. This conflict is particularly difficult to resolve in clear, oceanic waters, where UV radiation levels are high and camouflage is especially challenging. Reports of decreasing ozone levels at polar, temperate, and tropical latitudes (Solomon 1990; Stolarski et al. 1992) create an additional complication, because transparent zooplankton may face concomitant increases in UV radiation. A responsive increase in UV-protective pigmentation (at either an individual or population level) increases UV visibility, resulting in potentially increased predation or decreased feeding success. A responsive increase in depth may decrease access to prey, phytoplankton, or warm water.

The present study measures the UV and visible transparency of zooplankton and the waters they inhabit and relates these data to the ecologically relevant parameters of sighting distance and minimum attainable depth. Tissues from 15 epipelagic and 19 mesopelagic species of zooplankton from five phyla (Cnidaria, Ctenophora, Crustacea, Chaetognatha, and Chordata) were collected from three sites in the Northwest Atlantic Ocean. The transparency of various tissues was measured at wavelengths ranging from 280 to 500 nm. In addition, in situ measurements of downwelling irradiance from 330 to 500 nm were made at the site where all but two species of the epipelagic zooplankton were collected. These data were then related to sighting distance and minimum attainable depth using mathematical models based on contrast theory and the physics of light attenuation.

Materials and methods

Source of zooplankton and description of tissues examined

Zooplankton were obtained from the following three locations: Oceanographer Canyon (48°19′N; 68°08′W, on the southern edge of Georges Bank), Wilkinson Basin (42°30′N; 69°32′W, in the Gulf of Maine), and Woods Hole, Mass., USA. Zooplankton from Oceanographer Canyon and Wilkinson Basin were obtained during three cruises of the R.V. "Edwin Link" (July 1999, September 1999, June 2000). Approximately two-thirds of the mesopelagic zooplankton obtained during these cruises were collected at depth using the "Johnson Sea-Link" research submersible. These zooplankton were captured in 11-l plexiglass cylinders with hydraulically activated, sliding lids. The remaining mesopelagic zooplankton were collected using an opening/closing Tucker trawl (4.3 m^2 opening, 1/4 inch knotless nylon mesh) fitted with a thermally insulated collecting container that could be closed at depth. Over three-quarters of the epipelagic zooplankton were collected in glass jars using blue-water diving techniques (Hamner 1975; Johnsen and Widder 1998). The remaining zooplankton were collected using a surface plankton net (0.5 m^2 opening, 335 μm mesh). The lobate ctenophore *Mnemiopsis maccrydi* was obtained from the Aquatic Resources Division at the Marine Biological Laboratory (dipnetted from the surface in Woods Hole harbor). It and the cydippid ctenophore *Pleurobrachia pileus* (collected at the surface in Wilkinson Basin) were the only two epipelagic zooplankton not collected at Oceanographer Canyon. Although *M. maccrydi* and *P. pileus* were collected in water with considerably higher UV absorption than that found in Oceanographer Canyon, their location at the surface justifies their placement in the "high UV" epipelagic group.

Zooplankton were identified based on descriptions by Godeaux (1998) for salps, Kramp (1959) for medusae, and Wrobel and Mills (1998) for ctenophores. Table 1 lists the zooplankton collected, their dimensions, and depth of collection. All zooplankton were alive and in good condition at the time of measurement. Those collected on cruises were measured within an hour of collection. The ctenophore *M. maccrydi* was measured upon arrival.

Apparatus and procedure for measurement of UV and visible transparency

The apparatus used for measuring tissue transparency was modified from the one described by Johnsen and Widder (1998). The light source was a stabilized deuterium lamp (D-1000, Ocean Optics, Dunedin, Fla., USA) coupled to a 0.4 mm diameter fiber optic cable. The light exiting the fiber optic cable was collimated by a fused silica lens and reduced to a diameter of 3 mm by a fixed aperture. The beam passed through the specimen [held in a cuvette built from UV-transparent acrylic (Acrylite OP4, Cyro Industries, Mt. Arlington, N.J., USA)] and was focused onto a 1 mm diameter fiber optic cable by a second fused silica collimating lens. The light exiting the 1 mm cable was coupled to the detector of an optical multichannel analyzer (OMA-detector model 1420, detector interface model 1461, EG & G Princeton Applied Research) via a 25 μm slit. A fixed 3 mm diameter aperture was placed in front of the collection optics to limit the half-angle of acceptance of scattered light from the sample to 1°. The collimation and collection optics were kept in alignment using a precision metal frame designed for this purpose (74-ACH adjustable collimating lens holder, Ocean Optics). For further details on apparatus design, calibration, and operation, see Johnsen and Widder (1998).

Each specimen to be measured was placed in seawater in the UV-transparent cuvette. Five measurements through a given tissue were taken, followed by a reference measurement through the water. Each measurement consisted of an average of 50 consecutive 0.01 s exposures. The specimen was moved slightly between measurements to get an average value for the tissue measured. Percent transparency values for each wavelength were calculated by dividing the spectrum of the beam after passing through the tissue by the spectrum of the reference beam (that had passed through an equivalent distance of water).

In general, measurements were taken through the thickest non-opaque portion of the body (generally through extracellular matrix). All measurements were taken along an axis perpendicular to the longest axis of the specimen. Therefore, measurements of ctenophores were taken perpendicular to the oral–aboral axis; measurements of medusae were taken perpendicular to the plane of the bell; tunicate, crustacean, and chaetognath measurements were taken perpendicular to the anterior–posterior axis. More than one tissue was measured in several species that had large areas of different tissue types. All measurements were made on intact zooplankton, so a measurement through the muscle band of a salp, for example, was also through the test.

In order to compare more easily the degree of UV absorption among species, the transparency spectrum for each specimen was sometimes normalized by the percent transparency at 480 nm. This normalization also increased precision, because, while the transparency of different specimens of conspecific zooplankton varied with size, the relationship between the transparency values at two different wavelengths for a given measurement was quite constant (Johnsen and Widder 1998; present study). The transparency value at 480 nm was chosen because it usually approximated the average transparency in the visible range (Johnsen and Widder 1998) and because 480 nm is approximately the wavelength of peak sensitivity for many marine visual systems (Lythgoe 1972; Kirk 1983; Frank and Case 1988; Partridge et al. 1992). Finally, it also approximates the wavelength of maximum transmission in the ocean (Jerlov 1976).

In situ measurement of the penetration of downwelling UV irradiance

Depth profiles of the downwelling irradiance spectrum in Oceanographer Canyon were taken using a portable multichannel spectrometer (PS1000, Ocean Optics) operated from the rear dive chamber of the submersible. The spectrometer was optimized for maximum sensitivity by factory removal of the clad stripper and installation of a collection lens. The external fiber optic cable was a 1000 μm diameter silica fiber terminated with SMA connectors with O-ring seals. Two optical collectors were designed and tested: a diffuser with cosine response and an optically flat window. For the results reported here, only the flat window collector was used, because the poor flux transfer efficiency of the diffuser reduced sensitivity to such a degree that UV measurements were not possible. The flat window collector with the fiber optic had an in-water angular acceptance of 13°. The fiber optic light collector was mounted on a pan and tilt on top of the submersible along with an intensified video camera that ensured the field of view was free of obstructions such as ship shadow, ballast bubbles, etc.

Table 1 Dimensions of the collected zooplankton and the depth of collection (all given as mean ± SE). "Thickness" is the length of the light path through the individual. The salp *Cyclosalpa affinis* was an aggregate of seven individuals. Multiple conspecific individuals caught at one depth were included only once in the depth averages ([a]aggregate form, [b]bracts, [d]diameter of bell, [n]nectosome, [s]solitary form, [u]nurse)

Species	Thickness (mm)	Length (mm)	Depth (m)
Cnidaria			
Hydromedusae			
Aequorea forskalea Forskål (2)	16 ± 1	53 ± 3[d]	15
Botrynema brucei Browne (2)	15 ± 1	21 ± 1[d]	790 ± 10
Calycopsis sp. (typa and gara) Fewkes (2)	20 ± 0	20 ± 0	530 ± 80
Cunina globosa Eschscholtz (3)	6.7 ± 1	17 ± 3[d]	270 ± 3
Halicreas minimum Fewkes (3)	7.7 ± 2	26 ± 4[d]	550 ± 200
Orchistoma pileus Lesson (3)	11 ± 0.7	33 ± 3[d]	15
Pandea conica Quoy & Gaimard (2)	16 ± 0.5	29 ± 1	11
Ptychogena crocea Kramp & Damas (1)	17	20[d]	280
Solmissus incisus Fewkes (2)	18 ± 4	60 ± 20[d]	730 ± 20
Siphonophores			
Agalma okeni Eschscholtz (4)	12 ± 2[b]/17 ± 3[n]	81 ± 16	10 ± 2
Nanomia cara Agassiz (1)	10[b]/10[n]	45	340
Rosacea plicata Quoy & Gaimard (2)	18	120	280 ± 20
Scyphomedusae			
Aurelia aurita Linné (2)	13 ± 0	78 ± 3	12 ± 2
Pelagia noctiluca Forskål (1)	15	50	12
Ctenophora			
Beroids			
Beroe mitrata Moser (1)	8.0	15	15
Cestids			
Cestum veneris Lesueur (1)	3.0	300	15
Cydippids			
Euplokamis sp. Chun (2)	5.0 ± 0	21 ± 0.5	260
Pleurobrachia pileus Vanhöffen (2)	13 ± 1	17 ± 2	Surface
Lobates			
Bolinopsis infundibulum Muller (1)	20	45	500
Mnemiopsis maccrydi Mayer (11)	13 ± 1	25 ± 1	Surface
Ocyropsis maculata Rang (1)	35	40	150
Crustacea			
Hyperiid amphipods			
Cystisoma sp. Guerin-Meneville (1)	10	55	300
Decapods			
Pasiphaea multidentata Esmark (2)	2 ± 0	35 ± 3	200
Chaetognatha			
Sagitta hexaptera D'Orbigney (4)	3.3 ± 0.3	46 ± 2	170 ± 80
Sagitta maxima Conant (2)	3.0 ± 0	31 ± 2	250
Chordata			
Salps			
Cyclosalpa affinis Chamisso (2)[s]	24 ± 1	78 ± 8	9 ± 5
Cyclosalpa affinis Chamisso (1)[a]	60	60	15
Cyclosalpa polae Sigl (6)[a]	16 ± 0.5	37 ± 2	14
Iasis zonaria Pallas (4)[a]	9.3 ± 0.3	30 ± 1	300
Pegea confoederata Forskål (13)[a]	11 ± 0.6	30 ± 0.9	7.6 ± 4
Salpa aspera Chamisso (3)[s]	20 ± 1	78 ± 4	400 ± 60
Salpa cylindrica Cuvier (1)[s]	20	60	15
Salpa fusiformis Cuvier (10)[a]	13 ± 0.6	41 ± 1	280 ± 20
Thalia democratica Forskål (2)[s]	5.5 ± 0.5	15 ± 0.5	3
Doliolids			
Doliolina intermedium Neumann (1)[u]	10	25	500

The spectrometer was wavelength calibrated using a low pressure mercury spectrum lamp (HG-1 Mercury Argon Calibration Source, Ocean Optics) and intensity calibrated using an NIST (National Institute for Standards and Technology) referenced calibration source designed for the calibration of detectors from 350 to 800 nm (model OL310, Optronics Laboratories, Orlando, Fla., USA). Absolute intensity calibration was then performed by comparing the PS1000 value at 480 nm with the 480 nm value obtained using a self-calibrating radiometer (LoLAR; Widder et al. 1992) operated at the same depth (230 m) and time. Note that, although absolute irradiance values are not possible below 350 nm (due to the limits of the calibration source), relative irradiance levels (i.e. fraction of surface irradiance at a given depth) are possible, since the division creates dimensionless values. The noise limits of the spectrometer, however, limited relative irradiance levels to 330 nm and above. Relative irradiance at 320 nm was obtained by extrapolation, but values farther into the UVB range were unfortunately not possible. Because, the fiber optic light collector is not a true

cosine collector, it did not collect the increased oblique light present at deeper depths. Therefore, the calibration at 230 m slightly overestimates the downwelling irradiance at shallower depths.

Because the PS1000 spectroradiometer did not have the dynamic range to measure both deep and shallow spectra during the same dive, deep spectra were taken during midday dives, and shallow spectra were taken during sunset dives. The attenuation coefficients from the sunset, shallow measurements were then used to estimate the shallow values for midday dives.

Eight vertical profiles were taken during July 1999, and five were taken during June 2000. Due to Hurricanes Floyd and Gert, no profiles were taken during September 1999. Because all but two species of the epipelagic zooplankton were collected at Oceanographer Canyon, and because the two exceptions were collected at the surface (see above), depth profiles of UV radiation were only taken at this site.

Estimation of effects of UV absorption on sighting distance

The primary method of analysis in this and the following section compares the effect due to the measured UV transparency spectra to the effect due to a hypothetical flat spectrum $T(\lambda) = T(480)$ for all λ. Because the transparency spectra were commonly flat except for possible absorption in the UV range, this analysis estimates the effect of any UV absorption. The transparency value at 480 nm was chosen for the flat spectrum for the reasons previously described.

The sighting distance of an object is the distance at which its contrast drops below what a given viewer can detect. Because the sighting distance of a transparent zooplankter from an arbitrary viewpoint depends on its light scattering properties and the characteristics of the underwater light field (Chapman 1976), it is difficult to model exactly. In general, however, pelagic objects are most visible when viewed from below, and are often viewed from this angle (Mertens 1970; Munz 1990). For this viewing angle, Johnsen and Widder (1998) showed that the sighting distance at a wavelength λ is well approximated by:

$$d_{\text{sighting}}(\lambda) = \frac{\ln\left(\frac{C_{\min}(\lambda)}{1-\frac{T(\lambda)}{100}}\right)}{K(\lambda)-c(\lambda)}$$

where $C_{\min}(\lambda)$ is the minimum-contrast threshold for the viewer, and $K(\lambda)$ and $c(\lambda)$ are the diffuse and beam attenuation coefficients of the water. Note that, since $c(\lambda)$ is always greater than $K(\lambda)$, if $C_{\min}(\lambda) \geq 1 - \frac{T(\lambda)}{100}$, then $d_{\text{sighting}} = 0$, implying that the object is undetectable at any distance.

The sighting distance due to the measured transparency spectra (d_{sighting}) is compared to that due to the hypothetical flat spectra (d_{flat}) by forming the quotient:

$$\frac{d_{\text{sighting}}(\lambda)}{d_{\text{flat}}(\lambda)} = \frac{\ln\left(\frac{C_{\min}(\lambda)}{1-\frac{T(\lambda)}{100}}\right)}{\ln\left(\frac{C_{\min}(\lambda)}{1-\frac{T(480)}{100}}\right)}$$

Note that this quotient is independent of $K(\lambda)$ and $c(\lambda)$, and therefore independent of the optical characteristics of the water. The quotient was calculated for $C_{\min}$ values of 0.005 (best value reported for fish), 0.02 (human underwater vision under ideal conditions), 0.1, and 0.2 (an example of poor contrast vision) (Douglas and Hawryshyn 1990). The wavelength λ was set to be 360 nm, because almost all known UV visual pigments have sensitivity peaks $\geq$360 nm (reviewed by Douglas and Hawryshyn 1990 and Jacobs 1992). Because transparency was generally positively correlated with wavelength, using $\lambda = 360$ nm places an upper limit on $\frac{d_{\text{sighting}}}{d_{\text{flat}}}$.

While integrating contrast over the spectral range of a given UV visual pigment would theoretically provide a more accurate estimate of the effect on sighting distance than the value at one wavelength, this method requires knowledge of the wavelength dependence of c, K, and $C_{\min}$. The wavelength dependence of $C_{\min}$ is only known for a small number of species, and no currently available transmissometer measures c at UV wavelengths. Therefore, the above method provides the best estimate given current data and technology.

Estimation of effects of UV absorption on minimum attainable depth

An organism's exposure to UV radiation at a given depth and wavelength depends on the surface UV irradiance $U_s(\lambda)$, the diffuse attenuation coefficient $K(\lambda)$ of the water, and the fraction $P(\lambda)$ of the irradiance that reaches the upper surface of the organism that passes through to critical UV-sensitive tissues. Let $U_{\max}(\lambda)$ equal the maximum tolerable continuous intensity of UV radiation of wavelength λ for a given UV-sensitive tissue within an organism. Then,

$$U_{\max}(\lambda) = U_s(\lambda) \cdot e^{-K(\lambda)d_{\min}(\lambda)} \cdot P(\lambda)$$

where $d_{\min}(\lambda)$ is the minimum continuously tolerable depth for a given $U_{\max}(\lambda)$. Solving for $d_{\min}(\lambda)$ gives:

$$d_{\min}(\lambda) = \frac{\ln\left(\frac{U_{\max}(\lambda)}{U_s(\lambda)P(\lambda)}\right)}{-K(\lambda)}$$

The minimum attainable depth due to the measured transparency spectra ($d_{\min}$) is compared to that due to the hypothetical flat spectra (d_{flat}) by forming the difference:

$$d_{\text{flat}}(\lambda) - d_{\min}(\lambda) = \frac{\ln\left(\frac{U_{\max}(\lambda)}{U_s(\lambda)P(480)}\right)}{-K(\lambda)} - \frac{\ln\left(\frac{U_{\max}(\lambda)}{U_s(\lambda)P(\lambda)}\right)}{-K(\lambda)} = \frac{\ln\left(\frac{P(\lambda)}{P(480)}\right)}{-K(\lambda)}$$

Note that the difference is independent of $U_{\max}(\lambda)$ and $U_s(\lambda)$, and therefore independent of both the UV sensitivity of the tissue and the surface UV irradiance. Independence from these two parameters is important, because the first parameter is not known in general and the second varies over a large range. Factoring both out increases the generality of the results, but does not provide information on the minimum depths that the zooplankton can tolerate. The coefficient $K(\lambda)$ is taken from the vertical profiles of downwelling UV irradiance in Oceanographer Canyon. The fraction $P(\lambda)$ was estimated by the measured transparency $T(\lambda)$. Because $P(\lambda)$ is the fraction of irradiance (direct and oblique light) that reaches a given point, while the measured transparency $T(\lambda)$ is the fraction of radiance (direct light only) that reaches a given point, this approximation underestimates $P(\lambda)$ and thus puts an upper bound on the depth difference $d_{\text{flat}}(\lambda) - d_{\min}(\lambda)$. In this situation, however, oblique light likely contributes only a small fraction of the total irradiance. This is due to several factors. First, most of the light is contained in a small angular cone centered at some point between the location of the sun and the zenith (Jerlov 1976). Therefore, most of the light reaching the zooplankter arrives from one direction. Second, the majority of the tissues sampled attenuated only a moderate fraction of the light. This, coupled with the fact that most of the UV attenuation is likely due to absorption rather than scattering, implies that only a small fraction of photons within the tissue will be scattered into large oblique angles. The above factors allow one to roughly approximate $P(\lambda)$ with $T(\lambda)$. Note that the above analysis assumes that the critical UV-sensitive tissues are below the bulk of the zooplankter and thus places an upper limit on the decrease in minimum attainable depth.

Depth differences were calculated at wavelengths of 320 and 360 nm. The 360 nm wavelength was chosen because it is the central wavelength of the UVA range. The 320 nm wavelength was chosen because it was the only UVB wavelength for which good estimates of $K(\lambda)$ were available. While integrating radiation damage over a given damage action spectrum (e.g. Setlow, Robertson-Berger) theoretically provides a more accurate estimate of the effects on minimum attainable depth than the value at two wavelengths, this method is limited in practice for reasons similar to those described in the previous section.

The transparencies, sighting distances, and depth differences between mesopelagic and epipelagic tissues were compared using

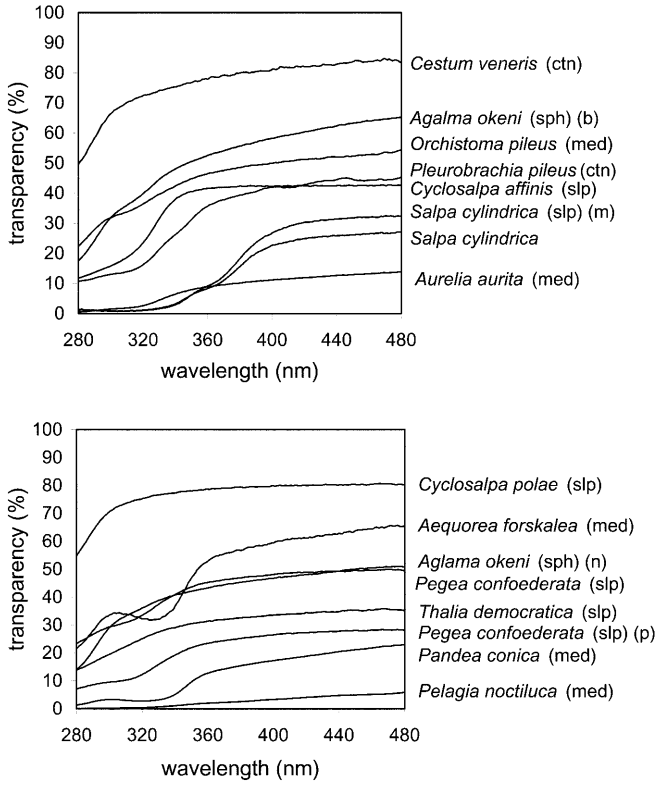

Fig. 1 Transmission spectra of tissues from epipelagic zooplankton. The transparency values of *Beroe mitrata* and the aggregate of *Cyclosalpa affinis* are too low to be shown on the graph and are omitted (*sph* siphonophore; *slp* salp; *b* bracts; *ctn* ctenophore; *m* muscle band; *med* medusa; *n* nectosome; *p* pigmented portion of test). The tissues are divided into two graphs and error bars are omitted for clarity

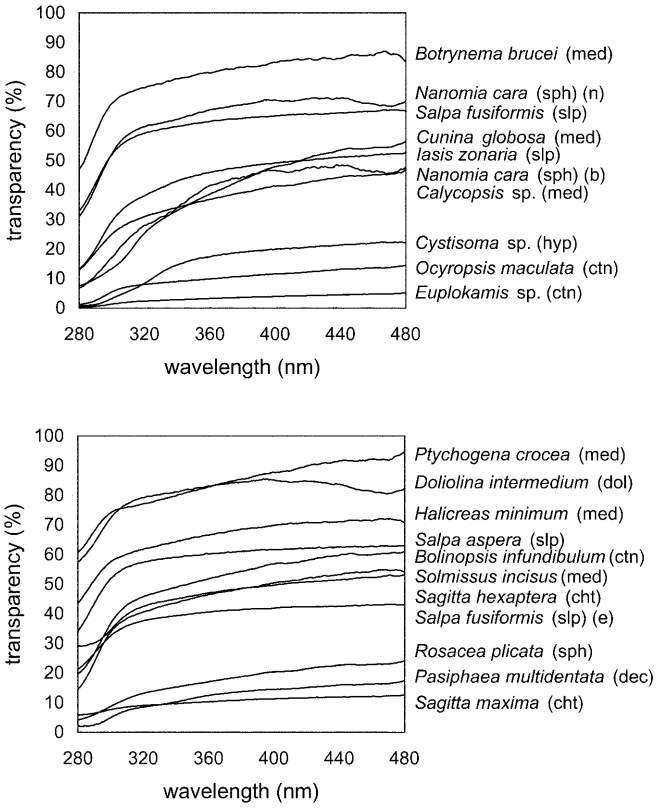

Fig. 2 Transmission spectra of tissues from mesopelagic zooplankton (*b* bracts; *cht* chaetognath; *ctn* ctenophore; *dec* decapod crustacean; *dol* doliolid; *e* endostyle; *hyp* hyperiid amphipod; *med* medusa; *n* nectosome; *slp* salp; *sph* siphonophore)

Student's *t*-test when the data were normally distributed with equal variances, and the Mann–Whitney rank sum test when either condition was not met. All statistics were performed using Sigmastat (Jandel Scientific).

Results

The epipelagic and mesopelagic zooplankton were collected at average depths of 11 ± 1 m ($n = 15$) and 370 ± 40 m ($n = 19$), respectively (all data are given as mean ± SE). The averaged percent transparency was plotted against wavelength for the epipelagic and mesopelagic tissues (Figs. 1, 2). Usually, percent transparency was approximately constant over most of the measured range, with a rapid decrease below a certain wavelength. In mesopelagic tissues, the cutoff wavelength was generally 300 nm, except for the hyperiid amphipod *Cystisoma* sp. In epipelagic tissues, the cutoff wavelength ranged from 300 to 400 nm. A few epipelagic tissues (e.g. *Agalma okeni* bracts, *Thalia democratica*, *Pelagia noctiluca*) and mesopelagic tissues (e.g. *Cunina globosa*, *Nanomia cara* bracts) did not have an obvious cutoff wavelength, but instead showed a steady and marked decrease in transparency with decreasing wavelength. Several epipelagic zooplankton (*Aequorea forskalea*, *Orchistoma pileus*, *Pandea conica*, *Pegea confoederata*) but no mesopelagic zooplankton had a secondary transparency maximum or shoulder at approximately 300 nm.

The average percent transparencies of the measured tissues from epipelagic and mesopelagic zooplankton at 480 nm were 38 ± 6 ($n = 19$) and 50 ± 6 ($n = 21$), respectively, and not significantly different ($P > 0.1$). The UV transparencies normalized by the 480 nm values were different, however, with epipelagic tissues showing lower transparency at UV wavelengths (Table 2; Fig. 3). Twelve out of 19 epipelagic tissues versus 4 of 21 mesopelagic tissues measured had normalized transparencies at 320 nm of ≤50%.

UV spectrum of downwelling light in Oceanographer Canyon

During a typical midday dive in July 1999, integrated downwelling UV irradiances (350–400 nm) were:

Depth (m)	Irradiance (photons cm^{-2} s^{-1})
30	2.3×10^{15}
44	6.9×10^{14}
66	5.4×10^{13}
81	1.9×10^{13}
92	6.5×10^{12}

Table 2 Transparency values of zooplankton at 480 nm and normalized transparencies at 400, 360, 320, and 280 nm. $T(480)$ is the percent transparency at 480 nm. $T(\lambda)/T(480)$ is the transparency at wavelength λ normalized by the transparency at 480 nm. When $n > 1$, the reported value is the average of the average values for each individual. When $n = 1$, the reported value is the average of the five measurements for that individual. The normalized transparency values [i.e. $T(\lambda)/T(480)$] are normalized before they are averaged [[a]aggregate of 7 individuals, [b]bracts, [e]endostyle, [m]muscle band, [n]nectosome, [p]pigmented portion of test; *superscripts preceding each species* refer to references confirming their placement as epipelagic or mesopelagic zooplankton: [1]Biggs (1976), [2]Madin (personal communication), [3]Margonski and Horbowa (1995), [4]Russell (1953), [5]Wrobel and Mills (1998), [6]Frank and Widder (personal communication), [7]Alvarino (1971), [8]Madin (1991), [9]Mayer (1912), [10]Kehayias et al. (1994), [11]Madin et al. (1996), [12]Deibel (1998), [13]Wiebe et al. (1979)]. Where a documented distribution includes both ranges, the range where the zooplankter was collected in the current study was chosen

	$T(480)$ (%)	$T(400)/T(480)$ (%)	$T(360)/T(480)$ (%)	$T(320)/T(480)$ (%)	$T(280)/T(480)$ (%)
Cnidaria					
Epipelagic					
[1]*Agalma okeni*[b]	65 ± 6	89 ± 2	80 ± 3	62 ± 6	26 ± 4
[1]*A. okeni*[n]	51 ± 9	91 ± 3	84 ± 4	70 ± 6	27 ± 7
[2]*Aequorea forskalea*	65 ± 3	91 ± 5	81 ± 10	50 ± 19	34 ± 11
[3]*Aurelia aurita*	14 ± 4	81 ± 2	64 ± 1	17 ± 5	3 ± 1
[2]*Orchistoma pileus*	54 ± 11	91 ± 2	84 ± 3	65 ± 6	39 ± 6
[4]*Pandea conica*	23 ± 0.3	75 ± 1	55 ± 1	12 ± 1	6 ± 0.4
[5]*Pelagia noctiluca*	6 ± 1	55 ± 2	33 ± 1	6 ± 0.4	1 ± 0.1
Mesopelagic					
[5]*Botrynema brucei*	83 ± 19	99 ± 3	95 ± 3	88 ± 5	55 ± 8
[2]*Calycopsis* sp.	47 ± 16	86 ± 8	74 ± 12	61 ± 16	23 ± 13
[2]*Cunina globosa*	56 ± 7	84 ± 4	67 ± 5	44 ± 4	13 ± 2
[5]*Halicreas minimum*	70 ± 4	97 ± 3	92 ± 4	85 ± 5	57 ± 9
[6]*Nanomia cara*[b]	48 ± 3	97 ± 1	87 ± 2	58 ± 5	14 ± 4
[6]*N. cara*[n]	70 ± 7	101 ± 1	96 ± 0.5	87 ± 1	44 ± 1
[4]*Ptychogena crocea*	97 ± 2	93 ± 0.4	89 ± 1	83 ± 1	65 ± 1
[7]*Rosacea plicata*	24 ± 8	80 ± 13	65 ± 16	48 ± 17	15 ± 7
[4]*Solmissus incisus*	54 ± 9	93 ± 1	86 ± 1	75 ± 1	26 ± 5
Ctenophora					
Epipelagic					
[5]*Beroe mitrata*	0.078 ± 0.03	83 ± 1	44 ± 4	6 ± 4	3 ± 3
[5]*Cestum veneris*	83 ± 2	97 ± 1	93 ± 1	87 ± 2	60 ± 3
[8]*Mnemiopsis maccrydi*	9 ± 2	75 ± 2	58 ± 2	31 ± 2	26 ± 2
[8]*Pleurobrachia pileus*	45 ± 11	92 ± 2	77 ± 9	32 ± 13	21 ± 12
Mesopelagic					
[5]*Bolinopsis infundibulum*	64 ± 2	93 ± 0.5	86 ± 1	76 ± 1	34 ± 1
[5]*Euplokamis* sp.	5 ± 1	78 ± 1	64 ± 0.2	46 ± 0.2	5 ± 0.2
[9]*Ocyropsis maculata*	14 ± 2	80 ± 1	68 ± 1	55 ± 1	8 ± 1
Crustacea					
Mesopelagic					
[2]*Cystisoma* sp.	22 ± 4	90 ± 2	78 ± 3	38 ± 2	3 ± 0.1
[6]*Pasiphaea multidentata*	16 ± 2	83 ± 0.3	71 ± 0.03	51 ± 2	20 ± 7
Chaetognatha					
Mesopelagic					
[10]*Sagitta hexaptera*	53 ± 10	91 ± 6	84 ± 9	74 ± 13	48 ± 19
[10]*Sagitta maxima*	19 ± 6	91 ± 2	84 ± 2	75 ± 3	51 ± 5
Choradata					
Epipelagic					
[11]*Cyclosalpa affinis*	43 ± 8	99 ± 1	97 ± 1	50 ± 27	25 ± 15
[11]*C. affinis*[a]	0.38 ± 0.08	84 ± 3	65 ± 4	10 ± 1	3 ± 0.2
[11]*Cyclosalpa polae*	80 ± 7	99 ± 1	98 ± 1	93 ± 2	67 ± 3
[5]*Pegea confoederata*	60 ± 7	98 ± 1	93 ± 2	75 ± 7	55 ± 7
[5]*P. confoederata*[p]	28 ± 1	94 ± 0.3	83 ± 0.3	43 ± 5	25 ± 3
[11]*Salpa cylindrica*	27 ± 9	80 ± 3	27 ± 4	4 ± 1	5 ± 1
[11]*S. cylindrica*[m]	32 ± 3	82 ± 1	28 ± 1	3 ± 0.1	4 ± 0.1
[5]*Thalia democratica*	35 ± 11	95 ± 3	88 ± 4	66 ± 18	33 ± 22
Mesopelagic					
[12]*Doliolina intermedium*	82 ± 1	104 ± 0.3	101 ± 0.1	96 ± 0.2	70 ± 6
[5]*Iasis zonaria*	52 ± 7	93 ± 2	87 ± 3	71 ± 4	24 ± 5
[13]*Salpa aspera*	63 ± 14	98 ± 1	95 ± 3	90 ± 4	52 ± 6
[11]*Salpa fusiformis*	67 ± 3	97 ± 1	95 ± 1	89 ± 1	49 ± 1
[11]*S. fusiformis*[e]	43 ± 1	98 ± 1	95 ± 1	88 ± 1	50 ± 4

The irradiance values below 370 and 380 nm at 81 and 92 m, respectively, were below the noise level of the spectrometer, and so were not included in the totals at those depths (Fig. 4A).

Using the midday spectra at 30 m and the sunset attenuation coefficient from 15 to 30 m, the midday downwelling UV irradiance at 11 m was estimated to be 9.2×10^{15} photons cm^{-2} s^{-1}. Approximately 40% of the surface downwelling irradiance at 330 nm and 80% at 400 nm remained at 11 m depth (Fig. 4B). Over 10% of the surface downwelling irradiance at 360 nm remained at 30 m, but <1% remained at 60 m.

The visible and UV diffuse attenuation coefficients were higher in June 2000 than in July 1999 (Fig. 5). The average attenuation coefficients at 360 nm in the 0–30 m depth interval were 0.08 ± 0.02 ($n = 8$) and 0.2 ± 0.02 m^{-1} ($n = 7$) during July 1999 and June 2000, respectively. The spectra were fit to polynomials to obtain values at 320 nm of 0.13 and 0.26 m^{-1} during July 1999 and June 2000.

The effects of UV absorption on sighting distance and minimum attainable depth

The effect of UV absorption on sighting distance was complex but generally correlated with increased visible transparency of the individual and decreased contrast sensitivity of the viewer (Fig. 6). With the exception of the highly transparent medusa *Ptychogena crocea*, the increases in sighting distance were uniformly small for viewers with good-contrast vision (2.8 ± 0.4% for $C_{min} = 0.005$, 4.1 ± 0.6% for $C_{min} = 0.02$). For viewers with poorer contrast vision, the increases were large in

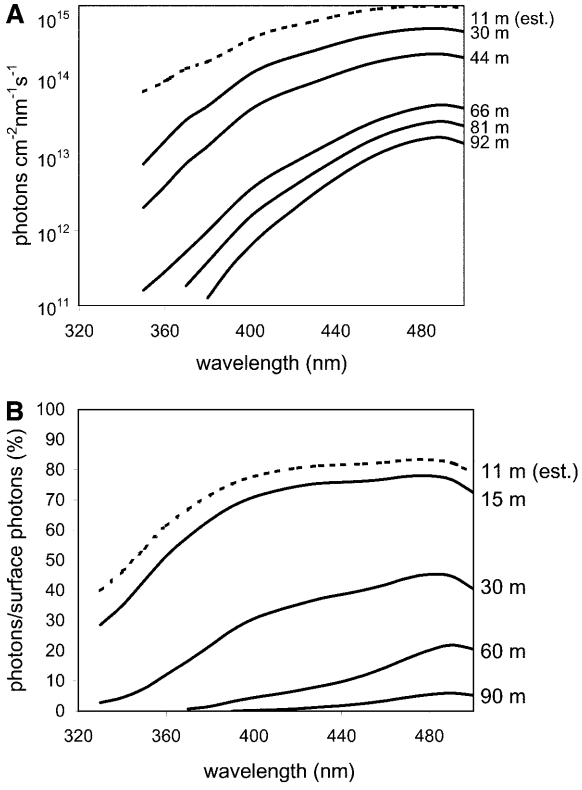

Fig. 4 **A** Downwelling irradiance in Oceanographer Canyon (dive 4141, 1053–1055 hours, 11 July 1999). There are no readings below 350 nm, because the spectrometer was not radiometrically calibrated below this wavelength. **B** Penetration of downwelling irradiance in Oceanographer Canyon (dive 4145, 1842–1855 hours, 12 July 1999). The relative spectra are normalized by a spectrum taken at 0 m (directly below the surface), where the downwelling UV irradiance was 2.8×10^{14} photons cm^{-2} s^{-1}. The relative spectra at 11 m (the average collection depth of the epipelagic zooplankton) were calculated based on the attenuation coefficient in the 0–15 m depth interval

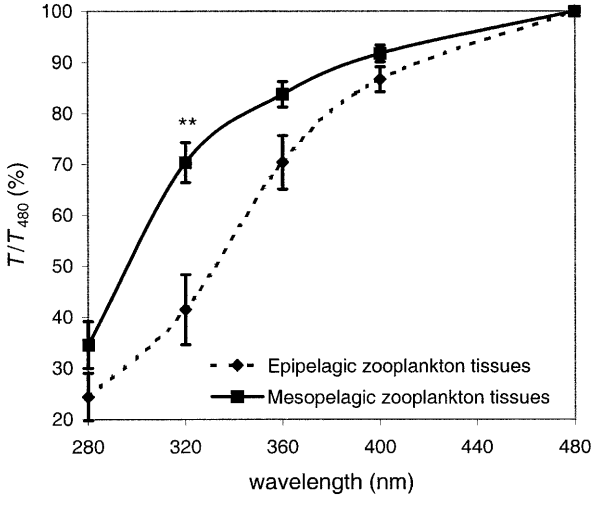

Fig. 3 Normalized UV transparency spectra of tissues from epipelagic and mesopelagic zooplankton (given as mean ± SE). Spectra are normalized by percent transparency at 480 nm and then averaged. $^{**}P < 0.005$. Note that while the difference at 360 nm is not significant, the P-value is quite low ($P = 0.056$)

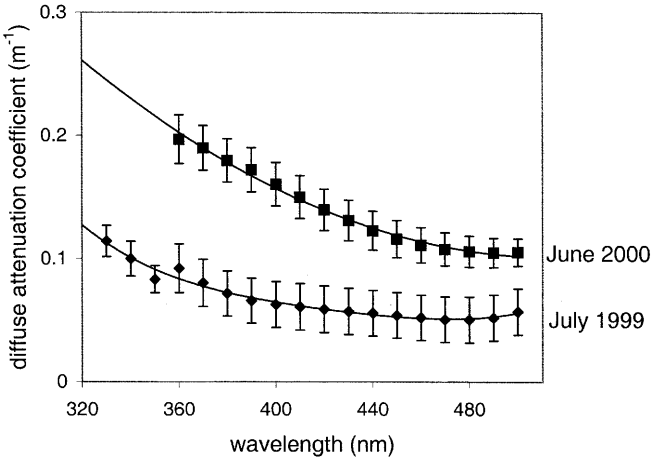

Fig. 5 Average diffuse attenuation coefficients in the 0–30 m depth interval calculated from vertical profiles of downwelling irradiance in Oceanographer Canyon during July 1999 and June 2000. Lines are polynomial fits to the data ($R^2 = 0.97$ for July 1999 fit; $R^2 = 0.99$ for June 2000 fit)

some instances (e.g. *Aequorea forskalea*, *Cunina globosa*, *Botrynema brucei*, *Halicreas minimum*, *Ptychogena crocea*, the bracts of *Aglama okeni*, *Cestum veneris*, *Cyclosalpa polae*, and *Salpa cylindrica*). When $C_{\min} = 0.2$, the increases in sighting distance for *B. brucei*, *P. crocea*, *C. veneris*, and *C. polae* could not be calculated because $d_{\text{flat}} = 0$. In these cases, UV absorption rendered the zooplankton detectable, where before they were undetectable at any distance. The doliolid *Doliolina intermedium* had a slightly higher transparency at 360 nm than at 480 nm, and so exhibited a small decrease in sighting distance. The tissues from the epipelagic and mesopelagic zooplankton did not have significantly different sighting distances for any of the minimum-contrast thresholds tested ($P > 0.5$ for all $C_{\min}$ values).

There was a marked and significant difference in decrease in minimum attainable depth between the tissues of epipelagic and mesopelagic zooplankton ($P < 0.0025$ for $\lambda = 320$ nm; $P < 0.05$ for $\lambda = 360$ nm) (Fig. 7). The decrease in minimum attainable depth was greater at 320 nm than at 360 nm ($P < 0.025$).

The zooplankton with the lowest increase in sighting distance (lowest cost) and highest decrease in minimum attainable depth (greatest benefit) had low visible transparency and high UV absorption and were generally epipelagic (Table 3). The zooplankton with the highest increase in sighting distance (highest cost) and lowest decrease in minimum attainable depth (lowest benefit) had high visible transparency and moderate UV absorption and were generally mesopelagic.

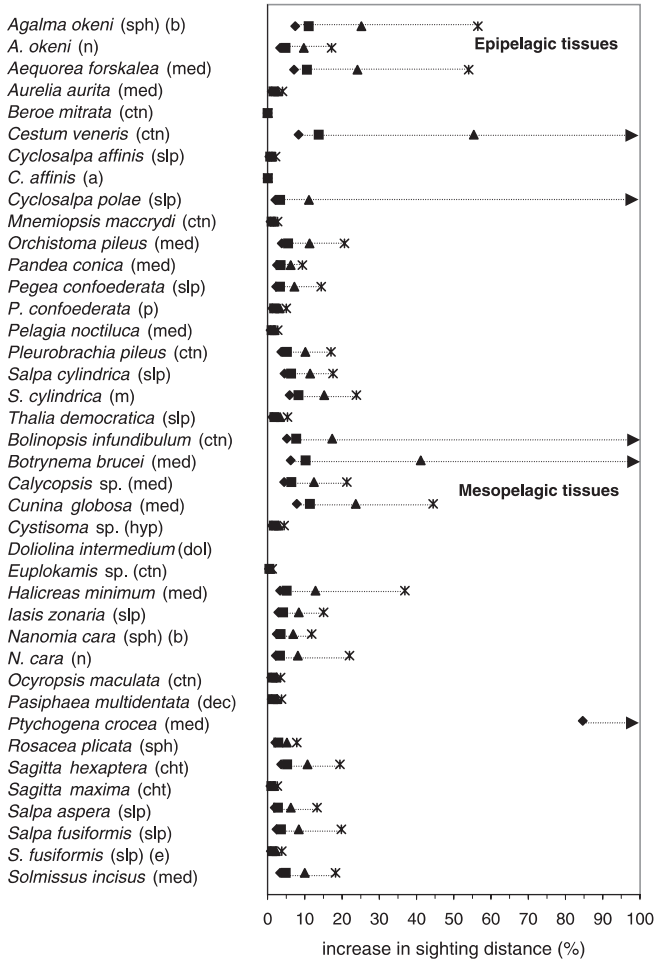

Fig. 6 Percentage increase in sighting distance due to measured transparency at 360 nm over that due to the hypothetical flat transparency spectrum $T(\lambda) = T(480)$ (◆⟶▶, $C_{\min} = 0.005$; ■, $C_{\min} = 0.02$; ▲, $C_{\min} = 0.1$; ∗, $C_{\min} = 0.2$). *Arrows* indicate where percentage increase could not be calculated; this occurs when the sighting distance for the hypothetical spectrum is zero, due to the fact that the inherent contrast (contrast at zero distance) of the target is below the minimum-contrast threshold of the viewer. In these cases, UV absorption renders the zooplankton detectable, where before they were not at any distance

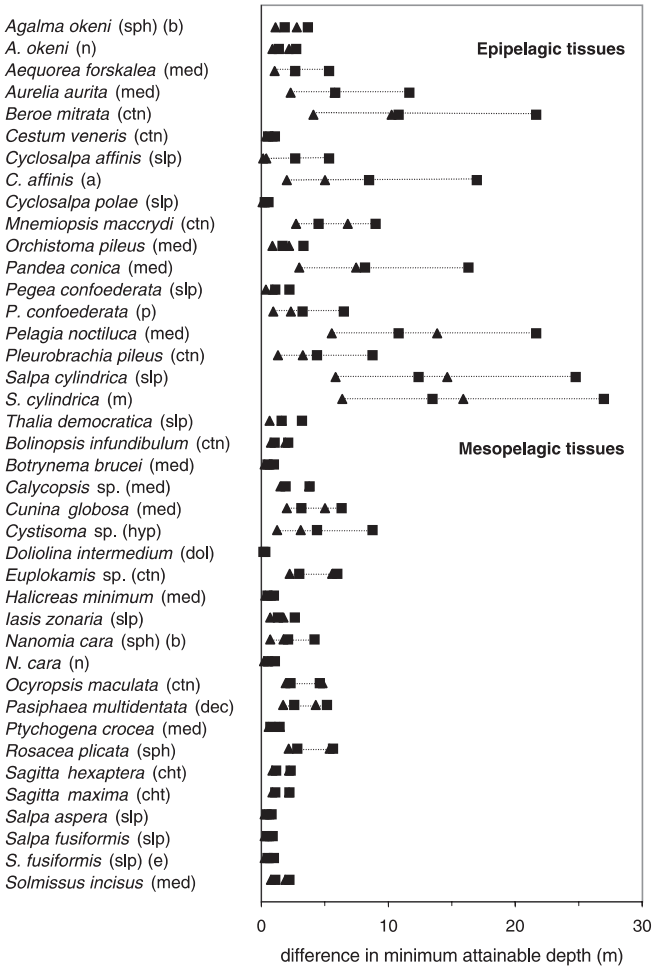

Fig. 7 Difference between minimum attainable depth due to measured transparency at 320 or 360 nm and that due to the hypothetical flat transparency spectrum $T(\lambda) = T(480)$ (■, difference when calculated at 320 nm; ▲, difference when calculated at 360 nm). The *left and right squares*/*triangles* for each tissue denote the depth difference determined using the averaged diffuse attenuation coefficients in the 0–30 m depth interval during June 2000 and July 1999, respectively

Table 3 Summary of cost/benefit analysis of UV absorption. Tissues are scored from 1 (best) to 3 (worst) on the effects of the measured UV absorption on UV visibility and minimum attainable depth. Visibility scores were determined by ranking the average sighting distance increases for each tissue. Depth scores were determined by ranking the average difference in minimum attainable depth at 320 nm for each tissue. Ranks 1–13 (lowest sighting distance increase or greatest depth difference) were given a score of 1, ranks 14–26 were given a score of 2, and ranks 27–40 (highest sighting distance increase or least depth difference) were given a score of 3. Total scores were determined by averaging the visibility and depth score and then ranking from 1 (best) to 5 (worst). Tissues within each total ranking are in alphabetical order. *Boldface type* indicates tissues from epipelagic zooplankton. *Plain type* indicates tissues from mesopelagic zooplankton

	Visibility score	Depth score	Total score
***Aurelia aurita* bell**	**1**	**1**	**1**
***Beroe mitrata* body**	**1**	**1**	**1**
***Cyclosalpa affinis* (a) test**	**1**	**1**	**1**
Cystisoma sp. thorax	1	1	1
Euplokamis sp. body	1	1	1
***Mnemiopsis maccrydi* body**	**1**	**1**	**1**
***Pelagia noctiluca* bell**	**1**	**1**	**1**
***Cyclosalpa affinis* test**	**2**	**1**	**2**
Ocyropsis maculata body	1	2	2
***Pandea conica* bell**	**2**	**1**	**2**
Pasiphaea multidentata thorax	1	2	2
***Pegea confoederata* pigmented test**	**2**	**1**	**2**
***Agalma okeni* nectosome**	**2**	**2**	**3**
Cunina globosa bell	3	1	3
Doliolina intermedium nurse	1	3	3
Iasis zonaria test	2	2	3
Nanomia cara bracts	2	2	3
***Pleurobrachia pileus* body**	**3**	**1**	**3**
Rosacea plicata bracts	2	2	3
Sagitta maxima body	1	3	3
***Salpa cylindrica* muscle band**	**3**	**1**	**3**
***Salpa cylindrica* test**	**3**	**1**	**3**
Salpa fusiformis endostyle	1	3	3
***Thalia democratica* test**	**2**	**2**	**3**
***Agalma okeni* bracts**	**3**	**2**	**4**
***Aequorea forskalea* bell**	**3**	**2**	**4**
Calycopsis sp. bell	3	2	4
***Cyclosalpa polae* test**	**2**	**3**	**4**
Nanomia cara nectosome	2	3	4
***Orchistoma pileus* bell**	**3**	**2**	**4**
***Pegea confoederata* test**	**2**	**3**	**4**
Sagitta hexaptera body	3	2	4
Salpa aspera test	2	3	4
Salpa fusiformis test	2	3	4
Solmissus incisus bell	2	3	4
Bolinopsis infundibulum body	3	3	5
Botrynema brucei bell	3	3	5
***Cestum veneris* body**	**3**	**3**	**5**
Halicreas minimum bell	3	3	5
Ptychogena crocea bell	3	3	5

Discussion

Visibility cost of UV absorption in epipelagic zooplankton

Relative to their transparency at 480 nm, many of the epipelagic zooplankton in this study were often considerably less transparent in the UV spectrum than were the mesopelagic zooplankton. While this absorption could potentially increase visibility to predators and prey with UV vision, the actual increases in sighting distance were generally minor. The reasons for this were twofold. First, with few exceptions, the UV absorption in the UVA range was small compared to the absorption in the UVB range. Because all known UV visual pigments operate in the UVA range (reviewed by Douglas and Hawryshyn 1990 and Jacobs 1992), the UV absorption measured in the present study generally had little effect on visibility. The minor effect of UV absorption on visibility was also due to the fact that most of the zooplankton with high UV absorption also had low transparency at visible wavelengths. The quotient $d_{\text{sighting}}/d_{\text{flat}}$ depended on UV absorption and visible transparency in a complex fashion. For less transparent zooplankton [low $T(480)$], $d_{\text{sighting}}/d_{\text{flat}}$ was linearly proportional to the degree of UV absorption and small even in cases of strong UV absorption. Therefore, zooplankton with high UV absorption did not necessarily have high increases in sighting distance (e.g. *Pandea conica*, *Beroe mitrata*).

For more transparent zooplankton [high $T(480)$], $d_{\text{sighting}}/d_{\text{flat}}$ was proportional to UV absorption, but in a non-linear fashion, with most of the cost incurred with slight absorption. Therefore, in highly transparent zooplankton even moderate UV absorption had a large effect on sighting distance. Because some highly transparent zooplankton had an inherent contrast (contrast at zero distance) less than the minimum-contrast threshold of a viewer with poor-contrast vision (Johnsen and Widder 1998; present study), they remained undetectable at any distance. For these zooplankton, the cost of UV absorption is potentially quite high because it can make them visible to species with poor-contrast sensitivity to which they would otherwise be undetectable.

Depth benefit of UV absorption in epipelagic zooplankton

Because many of the epipelagic zooplankton had significant UV absorption, their relevant UV exposure for a given depth may have been reduced. This implies that these species may tolerate shallower depths, thus increasing their depth range and access to prey, phytoplankton, or warmer water. The increases in depth range in Oceanographer Canyon were relatively high. While a decrease in minimum depth of 10–30 m is likely to be insignificant at mesopelagic depths, near the surface it potentially allows zooplankton to exploit regions with substantially different temperatures, salinities, and concentrations of predators, prey and phytoplankton. The effects may be more significant if UV-protective pigments are concentrated around critical tissues. If the critical tissues are small relative to the size of the zooplankter, the effect on visibility would be slight. This possibility is currently being addressed using UV video analysis.

The analysis in this study assumed that the critical UV-sensitive tissues were found on the ventral side of the organism. While this was true in certain cases (e.g.

certain medusae), it was certainly not true in general. Therefore, the estimated depth changes were upper limits. However, they can be generalized in the following way: suppose that $P(\lambda)$ and $P(480)$ are the fractions of light of wavelength λ and 480 nm that pass through an entire organism of thickness T. From the appendix:

$$\frac{p(\lambda,t)}{p(480,t)} = \frac{2-[2-\mathrm{P}(\lambda)]^{\frac{t}{T}}}{2-[2-\mathrm{P}(480)]^{\frac{t}{T}}}$$

where t is the distance of the UV-sensitive tissues from the upper surface of the zooplankter and $p(\lambda, t)$ and $p(480, t)$ are the fractions of incident light at wavelengths λ and 480 nm passing through to that distance. The ratio $p(\lambda, t)/p(480, t)$ ranges from unity when $t = 0$ (giving a depth difference of zero) to $P(\lambda)/P(480)$ (giving the depth difference presented in this study) when $t = T$. The form of the curve, however, depends on the transparency of the zooplankter. In highly transparent zooplankton [high $P(480)$], $p(\lambda, t)/p(480, t)$ is approximately linear in t. In less transparent zooplankton [low $P(480)$], $p(\lambda, t)/p(480, t)$ is non-linear in t, decreasing very slowly until t approaches T. In an inhomogeneous tissue, the relationship is more complex, but can be approached by mathematically dividing the tissue into regions of differing absorption.

Because UV absorption was invariably higher in the UVB than in the UVA range, the decrease in minimum attainable depth was greater for the former wavelength range. Both UVA and UVB are implicated in UV radiation damage (reviewed by Worrest 1982; El-Sayed et al. 1996; Meyer-Rochow 2000). However, although some forms of radiation damage (e.g. macular degeneration) appear to be caused primarily by UVA (Jacobs 1992), the majority of documented effects are due to UVB. Given this, and the fact that UV vision occurs in the UVA range, it is tempting to conclude that the high UVB absorption and lower UVA absorption measured in the epipelagic tissues in this study reflect an evolved compromise between the competing selective pressures of UV protection and UV concealment, particularly since certain transparent structures not used for camouflage (e.g. teleost ocular lenses) exhibit strong absorption across the entire UV range (Douglas and Thorpe 1992; Thorpe et al. 1993). This is premature, however, until more is known about the function and capabilities of marine UV visual systems and about the action spectra of UV radiation damage in transparent zooplankton, and until additional data on the diurnal, seasonal, and regional variation in depth ranges of zooplankton are available.

Due to the limits of the PS1000 spectrometer, the depth estimates are limited to $\lambda \geq 320$ nm. Because UVB extends from 280 to 320 nm, this study only examined the upper limit of this range. However, the data and the formulae from this study can be applied to in situ data from more sophisticated spectroradiometers to more fully examine the UVB spectrum.

Cause of decreased UV transparency in epipelagic zooplankton

The spectra of the epipelagic zooplankton strongly suggest that the decreased UV transparency was primarily due to increased absorption rather than increased scattering (see Johnsen and Widder 1998). The transparencies of the epipelagic and mesopelagic zooplankton at 280 and 480 nm were not significantly different, suggesting that the increased UV absorption in at least some the epipelagic zooplankton was not due to increased organic material, but to the presence of UV-protective compounds. While much is known about UV-protective compounds in phytoplankton, benthic organisms, and the lenses of teleosts (Yentsch and Yentsch 1982; Dunlap et al. 1991; Douglas and Thorpe 1992; Thorpe et al. 1993; Carroll and Shick 1996; Hannach and Sigelo 1998; Siebeck and Marshall 2001), little is known about such compounds in zooplankton (reviewed El-Sayed et al. 1996). Because different UV-protective pigments have characteristic spectra, the measured UV absorption spectra may be a valuable first step in identifying the compounds responsible (e.g. mycosporine-like amino acids, carotenoids, melanin).

It is likely that the UV absorption in some of the epipelagic zooplankton was not due to UV-protective pigments but to damage-inducing absorption by tissue. This had no effect on the visibility analysis, because visibility was increased by the same amount regardless of the source of the absorption. However, it may have affected the depth analysis if the damage-inducing absorption in the measured tissues represented a significant cost to the organism. The measured tissues were generally extracellular matrices, so the cost was likely to be small relative to the cost of UV absorption in cellular tissue and gonads. However, long-term exposure to UV radiation damage is known to reduce tissue transparency (reviewed by Meyer-Rochow 2000), adding yet another dimension to an already complex subject.

Acknowledgements We thank the captain and crew of the R.V. "Edwin Link" and the pilots and crew of the "Johnson Sea-Link" for assistance with all aspects of zooplankton collection. We also thank Dr. T. Frank for a critical reading of the manuscript, and Drs. L. Madin, and S. Haddock for help with species identifications. This work was funded by a grant from the National Science Foundation (OCE-9730073) to Drs. T.M. Frank and E.A.W., and by a Woods Hole Oceanographic Institution postdoctoral scholarship to S.J. This is Harbor Branch contribution no. 1367 and WHOI contribution no. 10251.

Appendix

Consider a tissue of thickness T that transmits fractions $P(\lambda_1)$ and $P(\lambda_2)$ of the incident light at wavelengths λ_1 and λ_2. Let $p(\lambda_1, t)$ and $p(\lambda_2, t)$ be the estimated fractions of a smaller thickness t of the same tissue. The problem is to find $p(\lambda_1, t)/p(\lambda_2, t)$ as a function of t, T, $P(\lambda_1)$ and $P(\lambda_2)$. First,

$$p(\lambda_1, t) = 1 - a(\lambda_1, t) \quad (1)$$

where $a(\lambda_1,t)$ is the fraction of light that has been removed from the beam. In a uniform tissue, light is attenuated exponentially. At zero thickness, the attenuation is nil. At thickness T, the attenuation is $A(\lambda_1) = 1 - P(\lambda_1)$. Therefore,

$$a(\lambda_1, t) = e^{kt} - 1 \quad (2)$$

and

$$A(\lambda_1) = e^{KT} - 1 \quad (3)$$

Solving Eq. 3 for k gives,

$$k = \frac{\ln[A(\lambda_1) + 1]}{T}$$

Substituting this into Eq. 2 gives,

$$a(\lambda_1, t) = e^{\frac{t}{T} \cdot \ln[A(\lambda_1)+1]} - 1 = [A(\lambda_1) + 1]^{\frac{t}{T}} - 1$$

Substituting this into Eq. 1 gives,

$$p(\lambda_1, t) = 1 - \left[[(1 - P(\lambda_1)) + 1]^{\frac{t}{T}} - 1\right] = 2 - [2 - P(\lambda_1)]^{\frac{t}{T}}$$

Since all the preceding arguments are valid for λ_2,

$$p(\lambda_2, t) = 2 - [2 - P(\lambda_2)]^{\frac{t}{T}}$$

and

$$\frac{p(\lambda_1, t)}{p(\lambda_2, t)} = \frac{2 - [2 - P(\lambda_1)]^{\frac{t}{T}}}{2 - [2 - P(\lambda_2)]^{\frac{t}{T}}}$$

References

Alvarino A (1971) Siphonophores of the Pacific with a review of the world distribution. University of California Press, Berkeley

Alldredge AL (1984) The quantitative significance of gelatinous zooplankton as pelagic consumers. In: Fasham MJR (ed) Flows of energy and materials in marine ecosystems. Plenum, New York, pp 407–434

Alldredge AL, Madin LP (1982) Pelagic tunicates: unique herbivores in the marine plankton. Bioscience 32: 655–663

Baier CT, Purcell JE (1997) Trophic interactions of chaetognaths, larval fish, and zooplankton in the South Atlantic Bight. Mar Ecol Prog Ser 146: 43–53

Biggs DC (1976) Nutritional ecology of *Agalma okeni*. In: Mackie GO (ed) Coelenterate ecology and behavior. Plenum, New York, pp 201–210

Bogenrieder A, Klein R (1982) Does solar UV influence the competitive relationship in higher plants? In: Calkins J (ed) The role of solar ultraviolet radiation in marine ecosystems. Plenum, New York, pp 641–649

Bothwell ML, Sherbot DMJ, Pollock CM (1994) Ecosystem response to solar ultraviolet-B radiation: influence of trophic level interactions. Science 265: 97–100

Bowmaker JK, Kunz YW (1987) Ultraviolet receptors, tetrachromatic color vision, and retinal mosaics in the brown trout (*Salmo trutta*): age-dependent changes. Vision Res 27: 2102–2108

Browman HI, Novales-Flamarique I, Hawryshyn CW (1994) Ultraviolet photoreception contributes to prey search behaviour in two species of zooplanktivorous fishes. J Exp Biol 186: 187–198

Buskey EJ, Mann CG, Swift E (1986) The shadow response of the estuarine copepod *Acartia tonsa*. J Exp Mar Biol Ecol 103: 65–75

Carleton KL, Harosi FI, Kocher TD (2000) Visual pigments of African cichlid fishes: evidence for ultraviolet vision from microspectrophotometry and DNA sequences. Vision Res 40: 879–890

Caron DA, Madin LP, Cole JJ (1989) Composition and degradation of salp fecal pellets: implications for vertical flux in oceanic environments. J Mar Res 47: 829–850

Carroll AK, Shick JM (1996) Dietary accumulation of UV-absorbing microsporine-like amino acids (MAAs) by the green sea urchin (*Strongylocentrotus droebachiensis*). Mar Biol 124: 561–569

Chalker-Scott L (1995) Survival and sex ratios of the intertidal copepod, *Tigriopus californicus*, following ultraviolet-B (290–320 nm) radiation exposure. Mar Biol 123: 799–804

Chapman G (1976) Reflections on transparency. In: Mackie GO (ed) Coelenterate ecology and behavior. Plenum, New York, pp 491–498

Coughlin DJ, Hawryshyn CW (1994) The contribution of ultraviolet and short-wavelength sensitive cone mechanisms to color vision in rainbow trout. Brain Behav Evol 43: 219–232

Cronin G, Hay ME (1995) Susceptibility to herbivores depends on recent history of both the plant and animal. Ecology 77: 1531–1543

Cronin TW, Frank TM (1996) A short-wavelength photoreceptor class in a deep-sea shrimp. Proc R Soc Lond Ser B Biol Sci 263: 861–865

Cronin TW, Marshall NJ, Quinn QA, King CA (1994) Ultraviolet photoreception in mantis shrimp. Vision Res 34: 1443–1452

Damkaer DM, Dey DB, Heron GA, Prentice EF (1980) Effects of UV-B radiation on near-surface zooplankton of Puget Sound. Oecologia 44: 149–158

Damkaer DM, Dey DB, Heron GA (1981) Dose/dose-rate responses of shrimp larvae to UV-B radiation. Oecologia 48: 178–182

Deibel D (1998) The abundance, distribution, and ecological impact of doliolids. In: Bone Q (ed) The biology of pelagic tunicates. Oxford University Press, New York, pp 171–186

Douglas RH, Hawryshyn CW (1990) Behavioral studies of fish vision: an analysis of visual capabilities. In: Douglas RH, Djamgoz MBA (eds) The visual system of fish. Chapman and Hall, New York, pp 373–418

Douglas RH, Thorpe A (1992) Short-wave absorbing pigments in the ocular lenses of deep-sea teleosts. J Mar Biol Assoc UK 72: 93–112

Dunlap WC, Banaszak AT, Rosenzweig TT, Shick J (1991) Ultraviolet light-absorbing compounds in coral reef holothurians: organ distribution and possible sources. In: Yanagisawa T, Yasumasu I, Oguro C, Suzuki N, Motokawa T (eds) Biology of Echinodermata: proceedings of the 7th international echinoderm conference. Balkema, Rotterdam, p 560

El-Sayed SZ, Van Dijken GL, Gonzalez-Rodas G (1996) Effects of ultraviolet radiation on marine ecosystems. Int J Environ Stud 51: 199–216

Fleischmann EM (1989) The measurement and penetration of ultraviolet radiation into tropical marine water. Limnol Oceanogr 34: 1623–1629

Forward RB (1976) A shadow response in a larval crustacean. Biol Bull (Woods Hole) 151: 126–140

Frank TM, Case JF (1988) Visual spectral sensitivities of bioluminescent deep-sea crustaceans. Biol Bull (Woods Hole) 175: 261–273

Frank TM, Widder EA (1996) UV light in the deep-sea: in situ measurements of downwelling irradiance in relation to the visual threshold sensitivity of UV-sensitive crustaceans. Mar Freshw Behav Physiol 27: 189–197

Godeaux J (1998) The relationships and systematics of the Thaliacea, with keys for identification. In: Bone Q (ed) The biology of pelagic tunicates. Oxford University Press, New York, pp 273–294

Goldsmith TH (1994) Ultraviolet receptors and color vision: evolutionary implications and dissonance of paradigms. Vision Res 34: 1479–1488

Greene CH (1983) Selective predation in freshwater zooplankton communities. Int Rev Gesamten Hydrobiol 68: 297–315
Häder DP, Worrest RC (1991) Effects of enhanced solar ultraviolet radiation on aquatic ecosystems. Photochem Photobiol 53: 717–725
Hamner WM (1975) Underwater observations of blue-water plankton: logistics, techniques and safety procedures for divers at sea. Limnol Oceanogr 20: 1045–1051
Hamner WM (1996) Predation, cover, and convergent evolution in epipelagic oceans. In: Lenz PH, Hartline DK, Purcell JE, Macmillan DL (eds) Zooplankton: sensory ecology and physiology. Overseas Publishers Association, Amsterdam, pp 17–37
Hamner WM, Madin LP, Alldredge AL, Gilmer RW, Hamner PP (1975) Underwater observations of gelatinous zooplankton: sampling problems, feeding biology, and behavior. Limnol Oceanogr 20: 907–917
Hannach G, Sigleo AC (1998) Photoinduction of UV-absorbing compounds in six species of marine phytoplankton. Mar Ecol Prog Ser 174: 207–222
Harbison GR, Madin LP, Swanberg NR (1978) On the natural history and distribution of oceanic ctenophores. Deep-Sea Res 25: 233–256
Hay ME (1996) Marine chemical ecology: what's known and what's next? J Exp Mar Biol Ecol 200: 103–134
Hobson ES, Chess JR (1978) Trophic relationships among fishes and plankton in the lagoon at Enewetok atoll, Marshall Islands. Fish Bull (Wash DC) 76: 133–153
Jacobs GH (1992) Ultraviolet vision in vertebrates. Am Zool 32: 544–554
Jerlov NG (1976) Marine optics. Elsevier, New York
Johnsen S (2000) Transparent animals. Sci Am 282: 62–71
Johnsen S, Widder EA (1998) The transparency and visibility of gelatinous zooplankton from the northwestern Atlantic and Gulf of Mexico. Biol Bull (Woods Hole) 195: 337–348
Karentz D (1994) Ultraviolet tolerance mechanisms in Antarctic marine organisms. In: Weiler CS, Penhale PA (eds) Ultraviolet radiation in Antarctica: measurements and biological effects. American Geophysical Union, Washington, DC, pp 93–110
Kehayias G, Fragopoulu N, Lykakis J (1994) Vertical community structure and ontogenetic distribution of chaetognaths in upper pelagic waters of the eastern Mediterranean. Mar Biol 119: 647–653
Kirk JTO (1983) Light and photosynthesis in aquatic ecosystems. Cambridge University Press, Cambridge
Kramp PL (1959) The hydromedusae of the Atlantic Ocean and adjacent waters. Dana-Rep Carlsberg Found 46: 1–283
Lalli CM, Gilmer RW (1989) Pelagic snails. Stanford University Press, Palo Alto
Loew ER, McFarland WN, Mills EL, Hunter D (1993) A chromatic action spectrum for planktonic predation by juvenile yellow perch, *Perca flavescens*. Can J Zool 71: 384–386
Losey GS, Cronin TW, Goldsmith TH, Hyde D, Marshall NJ, McFarland WN (1999) The UV visual world of fishes: a review. J Fish Biol 54: 921–943
Lythgoe JN (1972) The adaptation of visual pigments to their photic environment. In: Dartnall HJA (ed) Handbook of sensory physiology, vol VII/1. Springer, Berlin Heidelberg New York, pp 566–603
Madin LP (1991) Distribution and taxonomy of zooplankton in the Alboran Sea and adjacent western Mediterranean. Woods Hole Oceanogr Inst Tech Rep 26: 1–147
Madin LP, Kremer P, Hacker S (1996) Distribution and vertical migration of salps (Tunicata, Thaliacea) near Bermuda. J Plankton Res 18: 747–755
Madin LP, Purcell JE, Miller CB (1997) Abundance and grazing effects of *Cyclosalpa bakeri* in the subarctic Pacific. Mar Ecol Prog Ser 157: 175–183
Margonski P, Horbowa K (1995) Vertical distribution of cod eggs and medusae in the Bornholm basin. In: Thulin J, Frohlund K (eds) Scientific papers presented at the Polish–Swedish symposium on Baltic cod. Mir, Gdynia, Poland, pp 7–17
Marshall NJ, Oberwinkler J (1999) The colourful world of mantis shrimp. Nature 401: 873–874
Mayer AG (1912) Ctenophores of the Atlantic Coast of North America. Carnegie Institution, Washington, DC
McFall-Ngai MJ (1990) Crypsis in the pelagic environment. Am Zool 30: 175–188
McFarland WN (1991) Light in the sea: the optical world of elasmobranchs. J Exp Zool 5[Suppl]: 3–12
McFarland WN, Loew ER (1994) Ultraviolet visual pigments in marine fishes of the family Pomacentridae. Vision Res 34: 1393–1396
Mertens LE (1970) In-water photography: theory and practice. Wiley, New York
Meyer-Rochow VB (2000) Risks, especially for the eye, emanating from the rise of solar UV-radiation in the Arctic and Antarctic regions. Int J Circumpol Health 59: 38–51
Munz WRA (1990) Stimulus, environment and vision in fishes. In: Douglas RH, Djamgoz MBA (eds) The visual system of fish. Chapman and Hall, New York, pp 491–511
Odmark S, Wulff A, Waengberg SA, Nilsson C, Sundbaeck K (1998) Effects of UVB radiation in a microbenthic community of a marine shallow-water sandy sediment. Mar Biol 132: 335–345
Pages F, White MG, Rodhouse PG (1996) Abundance of gelatinous carnivores in the nekton community of the Antarctic polar frontal zone in summer 1994. Mar Ecol Prog Ser 141: 139–147
Partridge JC, Archer SN, Van Oostrum J (1992) Single and multiple visual pigments in deep-sea fishes. J Mar Biol Assoc UK 72: 113–130
Purcell JE (1997) Pelagic cnidarians and ctenophores as predators: selective predation, feeding rates and effects on prey populations. Ann Inst Oceanogr 73: 125–137
Russell FS (1953) The medusae of the British Isles. Cambridge University Press, Cambridge
Shashar N (1995) UV vision by marine animals: mainly questions. In: Gulko D, Jokiel PL (eds) Ultraviolet radiation and coral reefs: workshop on measurement of ultraviolet radiation in tropical coastal ecosystems. University of Hawaii Press, Honolulu, pp 201–206
Siebeck UE, Marshall NJ (2001) Ocular media transmission of coral reef fish – can coral reef fish see ultraviolet light? Vision Res 41: 133–149
Smith RC, Prézelin BB, Baker KS, Bidigare RR, Boucher NP, Coley T, Karentz D, MacIntyre S, Matlick HA, Menzies D, Ondrusek M, Wan Z, Waters KJ (1992) Ozone depletion: ultraviolet radiation and phytoplankton biology in Antarctic waters. Science 255: 952–959
Solomon S (1990) Progress toward a quantitative understanding of Antarctic ozone depletion. Nature 347: 347–354
Stolarski RS, Bojkov R, Bishop L, Zerefos C, Staehelin J, Zawodny J (1992) Measured trends in stratospheric ozone. Science 256: 342–349
Thorpe A, Douglas RH, Truscott RJW (1993) Spectral transmission and short-wave absorbing pigments in the fish lens. I. Phylogenetic distribution and identity. Vision Res 33: 289–300
Tovee MJ (1995) Ultra-violet photoreceptors in the animal kingdom: their distribution and function. Trends Ecol Evol 10: 455–460
Wängberg S, Selmer J, Gustavson K (1996) Effects of UV-B radiation on biomass and composition in marine phytoplankton communities. Sci Mar 60[Suppl 1]: 81–88
Widder EA, Caimi FM, Taylor LD, Tusting RF (1992) Design and development of an autocalibrating radiometer for deep sea biooptical studies. In: Proceedings of OCEANS '92, mastering the oceans through technology. Oceanic Engineering Society of the IEEE, New York, pp 525–530
Wiebe PH, Madin LP, Haury LR, Harbison GR, Philbin LM (1979) Diel vertical migration by *Salpa aspera* and its potential for large-scale particulate organic matter transport to the deep-sea. Mar Biol 53: 249–255
Worrest RC (1982) Review of literature concerning the impact of UV-B radiation upon marine organisms. In: Calkins J (ed) The role of solar ultraviolet radiation in marine ecosystems. Plenum, New York, pp 429–458

Wrobel D, Mills C (1998) Pacific coast pelagic invertebrates: a guide to common gelatinous animals. Monterey Bay Aquarium, Monterey Bay, Calif.

Yentsch CS, Yentsch CM (1982) The attenuation of light by marine phytoplankton with specific reference to the absorption of near-UV radiation. In: Calkins J (ed) The role of solar ultraviolet radiation in marine ecosystems. Plenum, New York, pp 691–700

Zaret TM, Kerfoot WC (1975) Fish predation on *Bosmina longirostris*: body size selection versus visibility selection. Ecology 56: 232–237